

Anomalous Josephson effect of s-wave pairing states in chiral double layers

Klaus Ziegler¹, Andreas Sinner¹, and Yurii E. Lozovik^{2,3}

¹ *Institut für Physik, Universität Augsburg, D-86135 Augsburg, Germany*

² *Institute of Spectroscopy, Russian Academy of Sciences, 142190 Troitsk, Moscow, Russia*

³ *Moscow Institute of Electronics and Mathematics, National Research University Higher School of Economics, 101000 Moscow, Russia*

(Dated: April 16, 2021)

We consider s-wave pairing in a double layer of two chiral metals due to Coulomb interaction, and study the Josephson effect near a domain wall, where the sign of the order parameter jumps. The domain wall creates two zero energy modes, whose superposition is associated with a current that flows in different direction in the two layers. Assuming a toroidal geometry, the effective Josephson currents winds around the domain walls, whose winding number is determined by the coefficients of the superimposed zero energy modes. This result can be understood as a competition of the conventional Josephson current perpendicular and the edge current parallel to a domain wall in a double layer of two chiral metals. As a realization we suggest the surface of a ring-shaped topological insulator. The duality between electron-electron and electron-hole double layers indicates that this effect should also be observable in excitonic double layers.

A Josephson junction is an important tool for probing paired electron states, since it is sensitive to the phase difference of the pairing order parameter on both sides of the junction. The latter generates a current that flows perpendicular to the Josephson junction. This effect has been studied in many systems with paired states, including conventional s-wave superconductors^{1,2}, unconventional and topological superconductors³⁻⁵.

In this paper we will consider the internal (intralayer) Josephson effect in a two-dimensional electronic double layer with interlayer s-wave pairing, assuming that both layers have a Dirac spectrum consisting of two bands and a spectral node (see Fig. 1). Such conditions can be realized, for instance, on the surface of a 3D topological insulator^{6,7}.

The nodal spectrum influences strongly the formation of local currents due to edge modes along the Josephson junction. They compete with the conventional Josephson current that tends to cross the junction perpendicularly. As a result we expect an anomalous Josephson effect, where the effective Josephson current has a component that flows parallel to the junction. The details of these competing effects will be studied in this paper. For this purpose the Josephson junction is simplified as a domain wall (i.e., it is an infinitesimally narrow Josephson junction). Zero energy edge modes are created along the domain wall, causing local currents. Finally, we impose periodic boundary conditions to obtain a toroidal geometry with two domain walls.

The theory of the electronic double layer is dual to that of an electron-hole double layer due to a duality transformation discussed previously by us¹⁰. This relation connects the electronic double layer physics with the excitonic physics. In particular, the duality suggests that the external (interlayer) Josephson effect should also exist for the electron-electron double layer when interlayer hopping is present, as it was studied before for electron-hole double layers^{8,9}. In that case the Josephson currents are homogeneous in each layer. In the present work this effect will not appear due to the absence of interlayer hopping. On the other hand, we expect an internal (intralayer) Josephson effect in electron-hole layers when we implement a Josephson junction inside the layers, as visualized in Fig. 1.

Model: We consider an electronic double layer with interlayer Coulomb repulsion but without interlayer tunneling. The layers themselves are chiral metals, described by Dirac Hamiltonians with opposite chirality. Such a system can be defined by the tight-binding Hamiltonian

$$\mathcal{H}_{ee} = \sum_{\mathbf{r}, \mathbf{r}'} \sum_{\mu, \mu'} (H_{\mathbf{r}\mathbf{r}', \uparrow, \mu \mu'} c_{\mathbf{r}, \uparrow, \mu}^\dagger c_{\mathbf{r}', \uparrow, \mu'} + H_{\mathbf{r}\mathbf{r}', \downarrow, \mu \mu'} c_{\mathbf{r}, \downarrow, \mu}^\dagger c_{\mathbf{r}', \downarrow, \mu'}) + \sum_{\mathbf{r}, \mathbf{r}'} \sum_{\mu, \mu'} V_{\mathbf{r}\mathbf{r}'} c_{\mathbf{r}, \uparrow, \mu}^\dagger c_{\mathbf{r}, \uparrow, \mu} c_{\mathbf{r}', \downarrow, \mu'}^\dagger c_{\mathbf{r}', \downarrow, \mu'} \quad (1)$$

where $\mu = 1, 2$ is the band index of the two bands in each layer. $H_{\mathbf{r}\mathbf{r}', \uparrow, \mu \mu'}$ ($H_{\mathbf{r}\mathbf{r}', \downarrow, \mu \mu'}$) is the hopping matrix element in the top (bottom) layer, and $c_{\mathbf{r}, \uparrow, \mu}^\dagger$ creates an electron at site \mathbf{r} in the top layer in the band with index μ . An example is the honeycomb lattice, which is bipartite and consists of two triangular sublattices. In this case $\mu = 1, 2$ refers to the two triangular lattices and the coordinate \mathbf{r} refers only to one of the two triangular lattices. There exists a duality transformation $c_{\mathbf{r}, \downarrow, \mu} \rightarrow d_{\mathbf{r}, \downarrow, \mu}^\dagger$ (i.e., we replace the electrons in the bottom layer by holes)¹⁰. The transformed Hamiltonian describes an electron-hole

double layer as

$$\begin{aligned} \mathcal{H}_{ee} \rightarrow \mathcal{H}_{eh} = & \sum_{\mathbf{r}, \mathbf{r}'} \sum_{\mu, \mu'} (H_{\mathbf{r}\mathbf{r}'} c_{\mathbf{r}, \uparrow, \mu}^\dagger c_{\mathbf{r}', \uparrow, \mu'} - H_{\mathbf{r}'\mathbf{r}} d_{\mathbf{r}, \downarrow, \mu}^\dagger d_{\mathbf{r}', \downarrow, \mu'}) - \sum_{\mathbf{r}, \mathbf{r}'} \sum_{\mu, \mu'} V_{\mathbf{r}\mathbf{r}'} c_{\mathbf{r}, \uparrow, \mu}^\dagger c_{\mathbf{r}, \uparrow, \mu} d_{\mathbf{r}', \downarrow, \mu'}^\dagger d_{\mathbf{r}', \downarrow, \mu'} \\ & + \sum_{\mathbf{r}, \mathbf{r}'} \sum_{\mu} V_{\mathbf{r}\mathbf{r}'} c_{\mathbf{r}, \uparrow, \mu}^\dagger c_{\mathbf{r}, \uparrow, \mu} + E_0, \end{aligned} \quad (2)$$

where the global energy shift is $E_0 = \sum_{\mathbf{r}} \sum_{\mu} H_{\mathbf{r}\mathbf{r}} c_{\mathbf{r}, \downarrow, \mu} c_{\mathbf{r}, \downarrow, \mu}$. \mathcal{H}_{eh} is the Hamiltonian of an electron-hole gas that interacts via an attractive Coulomb interaction. The electron-hole double layer has been studied intensively in terms of excitons^{8,11–18}.

Mean-field approximation: First, we briefly discuss the electron-hole double layer. Following the existing literature, we apply the BCS approach to this system. For this purpose we introduce the BCS order parameter

$$\Delta_{\mathbf{r}\mathbf{r}'; \mu\mu'} = V_{\mathbf{r}\mathbf{r}'} \langle c_{\mathbf{r}, \uparrow, \mu} d_{\mathbf{r}', \downarrow, \mu'} \rangle, \quad (3)$$

which describes Cooper pairing of electrons and holes by forming excitons⁸. Then the interaction term of \mathcal{H}_{eh} reads in BCS approximation

$$- \sum_{\mathbf{r}, \mathbf{r}'} \sum_{\mu, \mu'} V_{\mathbf{r}\mathbf{r}'} c_{\mathbf{r}, \uparrow, \mu}^\dagger c_{\mathbf{r}, \uparrow, \mu} d_{\mathbf{r}', \downarrow, \mu'}^\dagger d_{\mathbf{r}', \downarrow, \mu'} \approx - \sum_{\mathbf{r}, \mathbf{r}'} \sum_{\mu, \mu'} \left(d_{\mathbf{r}', \downarrow, \mu'}^\dagger c_{\mathbf{r}, \uparrow, \mu}^\dagger \Delta_{\mathbf{r}\mathbf{r}'} + h.c. \right).$$

A spatially uniform order parameter is obtained at temperature T as the minimum of the free energy

$$F_{MF} = -k_B T \log \text{Tr} e^{-\mathcal{H}_{MF}/k_B T}, \quad (4)$$

where mean-field (MF) condition $\delta_{\Delta} F = 0$ yields

$$\frac{1}{g} = \frac{1}{4} \int \frac{\tanh(\sqrt{E^2 + \Delta^2}/2k_B T)}{\sqrt{E^2 + \Delta^2}} \rho(E) dE \quad (5)$$

with the density of states $\rho(E)$ of the non-interacting model at the energy E . Here we have approximated the interaction as point-like, such that the corresponding inverse interaction strength reads as an integral over the Brillouin zone B :

$$\frac{1}{g} = \frac{1}{2|B|} \int_B \frac{1}{V_{\mathbf{p}}} d^2 p.$$

Quasiparticles are described by the corresponding Bogoliubov de Gennes Hamiltonian

$$\langle \mathcal{H}_{eh} \rangle \approx H_{BdG} = \begin{pmatrix} H_{\uparrow} & \Delta \\ \Delta^\dagger & -H_{\downarrow}^* \end{pmatrix}. \quad (6)$$

The analog MF approximation can be applied to the electron-electron Hamiltonian H_{ee} . It results in

$$\sum_{\mathbf{r}, \mathbf{r}'} \sum_{\mu, \mu'} V_{\mathbf{r}\mathbf{r}'} c_{\mathbf{r}, \uparrow, \mu}^\dagger c_{\mathbf{r}, \uparrow, \mu} c_{\mathbf{r}', \downarrow, \mu'}^\dagger c_{\mathbf{r}', \downarrow, \mu'} \approx \sum_{\mathbf{r}, \mathbf{r}'} \sum_{\mu, \mu'} \left(\Delta_{\mathbf{r}\mathbf{r}'; \mu\mu'} c_{\mathbf{r}, \uparrow, \mu}^\dagger c_{\mathbf{r}', \downarrow, \mu'} + h.c. \right)$$

with the pairing order parameter

$$\Delta_{\mathbf{r}\mathbf{r}'; \mu\mu'} = V_{\mathbf{r}\mathbf{r}'} \langle c_{\mathbf{r}, \uparrow, \mu} c_{\mathbf{r}', \downarrow, \mu'}^\dagger \rangle. \quad (7)$$

Then the effective quasiparticle Hamiltonian reads

$$\langle \mathcal{H}_{ee} \rangle \approx H_{MF} = \begin{pmatrix} H_{\uparrow} & \Delta \\ \Delta^\dagger & H_{\downarrow} \end{pmatrix}, \quad (8)$$

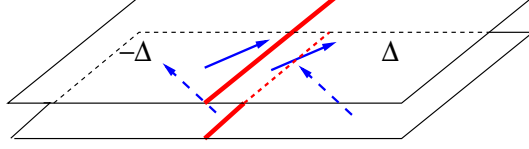


FIG. 1: Electronic double layer with domain wall, which is given by a sign jump of the pairing order parameter. The currents (blue arrows) flow in the same (opposite) direction in the two layers parallel (perpendicular) to the domain wall.

which becomes for two layers with opposite chiralities

$$H_{MF} = \begin{pmatrix} h_1\sigma_1 + h_2\sigma_2 & \Delta\sigma_2 \\ \Delta\sigma_2 & h_1\sigma_1 - h_2\sigma_2 \end{pmatrix}, \quad (9)$$

where we have assumed that the hopping elements h_1 and h_2 are the same in both layers. σ_j is the Pauli matrix with respect to the sublattice structure, and Δ is a real scalar pairing order parameter. In Fourier representation $h_{1,2}$ and Δ can depend on the 2D wave vector $\mathbf{k} = (k_1, k_2)$. The gapped quasiparticle dispersion of H_{MF} reads $E_{\mathbf{k}} = \pm\sqrt{h_1^2 + h_2^2 + \Delta^2}$. The latter agrees with the dispersion of the Hamiltonian with identical layers¹⁰

$$H_{MF0} = \begin{pmatrix} h_1\sigma_1 + h_2\sigma_2 & \Delta\sigma_3 \\ \Delta\sigma_3 & h_1\sigma_1 + h_2\sigma_2 \end{pmatrix}. \quad (10)$$

Thus, the difference of these two Hamiltonians can only be seen in the eigenfunctions but not in their spectra.

The dispersion $E_{\mathbf{k}} = \pm\sqrt{h_1^2 + h_2^2 + \Delta^2}$ vanishes when h_1 or h_2 are imaginary. This is the case for evanescent modes. The phenomenon is known from conventional Josephson junctions, where evanescent modes exist inside the gap.

Zero modes at a domain wall: An inhomogeneous order parameter Δ breaks translational invariance and divides the layers in different regions with either positive or negative Δ . Here we will consider the case in which only the sign of Δ changes in space but $|\Delta|$ is uniform. For a Josephson junction¹ we typically choose a region around $x = 0$, where the order parameter vanishes. For our purpose we can consider the simple case^{19,20} that $\text{sgn}(\Delta)$ jumps at the domain wall along the y direction at $x = 0$, as visualized in Fig. 1. Such a discontinuous phase change suppresses the Andreev states except for the zero modes. It should be kept in mind here that the domain wall is created by a potential, and the corresponding change of the order parameter should be obtained via the BCS-like equation. In practice, this requires some tedious calculations and we simply focus here on the domain wall in terms of $\Delta(x)$, following the recipe proposed in Ref. [19]. Next, we analyze the effect of the domain wall on the low energy MF Hamiltonian with $h_1 \sim i\partial_x$, $h_2 \sim k_2$

$$H_{MF} = \begin{pmatrix} i\partial_x\sigma_1 + h_2\sigma_2 & \Delta(x)\sigma_2 \\ \Delta(x)\sigma_2 & i\partial_x\sigma_1 - h_2\sigma_2 \end{pmatrix}. \quad (11)$$

For the zero mode we can make the ansatz $\Psi_{k_2}(x) = \psi_{k_2}e^{-bx}$, where b depends on the sign of x . Then we get the eigenmode equations

$$H_{MF}\Psi_{k_2}(x) = \begin{pmatrix} -ib\sigma_1 + h_2\sigma_2 & \Delta(x)\sigma_2 \\ \Delta(x)\sigma_2 & -ib\sigma_1 - h_2\sigma_2 \end{pmatrix}\Psi_{k_2}(x) = 0. \quad (12)$$

Using the matching condition at $x = 0$, the evanescent solutions require $b = \text{sgn}(x)\sqrt{h_2^2 + \Delta^2}$ and $h_2 = 0$, such that $b = \text{sgn}(x)|\Delta|$ and the zero modes read

$$\Psi_1 = \frac{1}{\mathcal{N}} \begin{pmatrix} 1 \\ 0 \\ 1 \\ 0 \end{pmatrix} e^{-|\Delta||x|}, \quad \Psi_2 = \frac{1}{\mathcal{N}} \begin{pmatrix} 0 \\ 1 \\ 0 \\ -1 \end{pmatrix} e^{-|\Delta||x|} \quad (13)$$

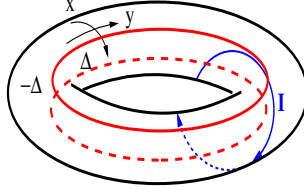


FIG. 2: After gluing the double layer to form a torus, the current \mathbf{I} winds along the two domain walls around the torus.

with the normalization $\mathcal{N} = \sqrt{2/|\Delta|}$. Ψ_1 has the same wavefunction on the top and the bottom layer, whereas Ψ_2 has an opposite sign on the two layers.

Symmetries and zero modes: The characteristic polynomial of the MF Hamiltonian has four degenerate zero solutions for $h_2 = 0$ and $b(x) = \text{sgn}(x)|\Delta|$. We consider the block-diagonal matrices $S_j = \text{diag}(\sigma_j, \sigma_j)$ and $T_j = \text{diag}(\sigma_j, -\sigma_j)$ for $j = 1, 2, 3$. First, for $h_2 = 0$ the MF Hamiltonian is invariant under the transformation $H \rightarrow T_1 H_{MF} T_1$, which creates a new zero mode from Ψ_1 with $\Psi_2 = T_1 \Psi_1$. Moreover, $T_2 = \text{diag}(\sigma_2, -\sigma_2)$ is a particle-hole transformation, since $T_2 H_{MF} T_2 = -H_{MF}$ and $H_{MF} T_2 \Psi_E = -E T_2 \Psi_E$. Thus, T_1 and T_2 create from Ψ_1 three more zero modes. In particular, the fact that the transformation matrices obey the following rules

$$S_j^2 = T_j^2 = \mathbf{1}, \quad T_1 T_2 = S_1 S_2 = i S_3 \quad (14)$$

and $S_3 \Psi_1 = \Psi_1$, $T_2 \Psi_1 = i \Psi_2$ and $T_2 T_1 \Psi_1 = S_2 S_1 \Psi_1 = i \Psi_1$ reflects that the zero energy is an exceptional point with a two-dimensional eigenspace²¹. It should be noted that the zero eigenmodes of H_{MF} are real. But any superposition of the two zero modes $\Phi = a_1 \Psi_1 + a_2 \Psi_2$ with complex coefficients $a_j = |a_j| e^{i\varphi_j}$ and normalization $|a_1|^2 + |a_2|^2 = 1$ is also a zero mode.

Since both zero eigenmodes decay exponentially with $|x|$, they are both physically valid. Thus, for a unique solution at zero energy we need an extra condition. The y direction does not select physical valid solutions because we need $h_2 = 0$; i.e., the solution must be constant in that direction, which can only be satisfied by periodic boundary conditions. A possible solution is to impose a condition on the physical properties, for instance, by fixing the current density. This will be discussed subsequently.

Currents: The current densities induced by the zero modes are expressed separately for the top and for the bottom layer, where we have the wavefunctions

$$\Phi_{\uparrow} = \begin{pmatrix} a_1 \\ a_2 \end{pmatrix} \frac{e^{-|\Delta||x|}}{\mathcal{N}}, \quad \Phi_{\downarrow} = \begin{pmatrix} a_1 \\ -a_2 \end{pmatrix} \frac{e^{-|\Delta||x|}}{\mathcal{N}}. \quad (15)$$

Using the continuity equation²², we get for the top layer

$$\partial_t \Phi_{\uparrow} \cdot \Phi_{\uparrow} - \partial_x j_{x\uparrow} = \Delta(x) \Phi_{\uparrow} \cdot \sigma_2 \Phi_{\downarrow} \quad (16)$$

and for the bottom layer

$$\partial_t \Phi_{\downarrow} \cdot \Phi_{\downarrow} - \partial_x j_{x\downarrow} = \Delta(x) \Phi_{\downarrow} \cdot \sigma_2 \Phi_{\uparrow}. \quad (17)$$

The current densities are related to the current operator $\frac{e}{i\hbar} [H_{MF}, r_{\mu}]$, projected onto the top or bottom layer, respectively:

$$j_{x\uparrow} = -j_{x\downarrow} = |\Delta| |a_1 a_2| \cos(\varphi_2 - \varphi_1) e^{-2|\Delta||x|}. \quad (18)$$

Since the wavefunction is constant with respect to the y component, the corresponding current densities

$$j_{y\uparrow} = j_{y\downarrow} = |\Delta| |a_1 a_2| \sin(\varphi_2 - \varphi_1) e^{-2|\Delta||x|} \quad (19)$$

do not appear in the continuity equations. The properties $j_{y\uparrow} = j_{y\downarrow}$ ($j_{x\uparrow} = -j_{x\downarrow}$) reflect the fact that the currents in the two layer are (anti-) correlated (cf. Fig. 1). This effect should be experimentally observable, since the interlayer current-current correlation is associated with the drag effect^{10,23}.

A non-vanishing current requires that both zero modes contribute (i.e. $a_1, a_2 \neq 0$). The currents of the two layers in y direction are not balanced in contrast to the currents in x direction; i.e., they do not cancel each other in the two layers. Thus, there is a net current along the y direction in the double layer (cf. Fig. 1). Since the layers are charge separated, there is no charge current between them. Therefore, the currents must be conserved in each layer. The fact that the quasiparticle currents $j_{x,\uparrow}, j_{x,\downarrow}$ are not conserved inside an individual layer reflects the existence of a current carried by Cooper pairs²² (“supercurrent”).

The picture in Fig. 1 is incomplete though because the boundaries of the layers have not been included. We can introduce periodic boundary conditions in x and y direction, resulting in the toroidal geometry of Fig. 2. It provides also the condition to maintain a unique solution of the zero mode, since the winding number m of the current must be an integer for a torus with major (minor) circumference L (M):

$$j_{y,\uparrow}/j_{x,\uparrow} = \tan(\varphi_2 - \varphi_1) = L/mM . \quad (20)$$

Thus, the value of m fixes the phase difference $\varphi_2 - \varphi_1$ of the coefficients a_1, a_2 , while $|a_1 a_2|$ is linked to the values of the current components due to Eqs. (18), (19).

Preparing the wavefunction $\Phi = (\Phi_\uparrow, \Phi_\downarrow)$ we create a current density $(j_{x,\uparrow}, j_{y,\uparrow})$ in the top and $(-j_{x,\uparrow}, j_{y,\uparrow})$ in the bottom layer. By changing the wavefunction Φ through the coefficients a_j these current densities also change according to the above relations. This change can be achieved experimentally with an external current source that couples inductively to the double layer. By choosing the direction of the current (i.e., the angle $\varphi_2 - \varphi_1$), we excite the corresponding wave function Φ .

Discussion: The existence of edge modes, a consequence of the chiral metallic layers, affects the Josephson currents near the domain wall. A measure of the competition between the conventional Josephson current and the edge current is the winding number m of the helical current around the domain walls in Fig. 2. Such edge modes appear on all edges including the sample boundaries. In Fig. 1 the latter have not been depicted because an infinite 2D sample was assumed. On the other hand, it is well known that a consistent description of edge modes requires a compact manifold²⁰. Fig. 2 presents a compact version of the double layer as a single layer on a torus (i.e., for periodic boundary conditions), which has two domain walls. Such a geometry can be realized as the surface of a ring-shaped topological insulator.

The existence of two degenerate zero modes requires an additional physical constraint to lift the degeneracy and to obtain a unique solution. In our case this was achieved by considering the current in the sample. Depending on that current we get a specific linear combination of the two zero modes. From a physical perspective this means that we induce a current density in the system by coupling to an external current, which excites the corresponding quasiparticle state. The exponential decay of quasiparticle modes and their corresponding currents away from the domain walls on the scale $1/|\Delta|$ implies the existence of a supercurrent due to charge conservation²². In other words, the quasiparticle currents near the domain wall are part of a stationary current inside the entire torus, winding around the domain walls (cf. Fig. 2). This current, which is proportional to $|\Delta|$, could be measured through inductance, e.g., by using a coil. Very accurate measurements of the current can be performed with a SQUID²⁴. A more direct probe of the zero modes would be possible with an electronic Mach-Zehnder interferometer^{25,26}.

Our calculation was performed for the special example of a jump of the order parameter phase. Similar calculations can be done for other shapes of $\Delta = |\Delta|e^{i\alpha(x)}$, provided that the order parameter phase represents a kink with a global phase change π from one boundary to the other in x direction. Although the anomalous Josephson effect will not be changed qualitatively, the decay of the wavefunctions and of the current densities might be different. In particular, a broader Josephson junction might have different modes (cf. discussion in Ref. [27]).

In conclusion, we found an anomalous Josephson current caused by the superposition of two zero energy modes in the vicinity of the domain wall. The direction of this current is determined by the coefficients of the superposition. Conversely, an external current in a specific direction can induce a certain superposition of the zero modes on the surface of a ring-shaped topological insulator.

Acknowledgments:

This research was supported by a grant of the Julian Schwinger Foundation for Physics Research. Yu.E.L. was supported through the grants RFBR 20-02-00410 and 20-52-00035.

-
- ¹ B. Josephson, *Physics Letters* **1**, 251 (1962), ISSN 0031-9163, URL <http://www.sciencedirect.com/science/article/pii/0031916362913690>.
 - ² P. W. Anderson and J. M. Rowell, *Phys. Rev. Lett.* **10**, 230 (1963), URL <https://link.aps.org/doi/10.1103/PhysRevLett.10.230>.
 - ³ Y. Tanaka, T. Hirai, K. Kusakabe, and S. Kashiwaya, *Phys. Rev. B* **60**, 6308 (1999), URL <https://link.aps.org/doi/10.1103/PhysRevB.60.6308>.
 - ⁴ Y. Asano, Y. Tanaka, M. Sigrist, and S. Kashiwaya, *Phys. Rev. B* **67**, 184505 (2003), URL <https://link.aps.org/doi/10.1103/PhysRevB.67.184505>.
 - ⁵ H.-J. Kwon, K. Sengupta, and V. M. Yakovenko, *The European Physical Journal B - Condensed Matter and Complex Systems* **37**, 349 (2004), ISSN 1434-6036, URL <https://doi.org/10.1140/epjb/e2004-00066-4>.
 - ⁶ X.-L. Qi and S.-C. Zhang, *Rev. Mod. Phys.* **83**, 1057 (2011), URL <https://link.aps.org/doi/10.1103/RevModPhys.83.1057>.
 - ⁷ A. A. Burkov, *Journal of Physics: Condensed Matter* **27**, 113201 (2015), URL <https://doi.org/10.1088/0953-8984/27/11/113201>.
 - ⁸ Y. E. Lozovik and V. I. Yudson, *Soviet Journal of Experimental and Theoretical Physics* **44**, 389 (1976).
 - ⁹ Y. E. Lozovik and A. V. Poushnov, *Physics Letters A* **228**, 399 (1997), ISSN 0375-9601, URL <https://www.sciencedirect.com/science/article/pii/S0375960197001333>.
 - ¹⁰ A. Sinner, Y. E. Lozovik, and K. Ziegler, *Physical Review Research* **2**, 033085 (2020), 1912.13257.
 - ¹¹ B. Halperin and R. Englman, *Solid State Communications* **66**, 711 (1988), ISSN 0038-1098, 25th Anniversary Year, URL <http://www.sciencedirect.com/science/article/pii/0038109888909891>.
 - ¹² J. P. Eisenstein and A. H. MacDonald, *Nature* **432**, 691 (2004), ISSN 1476-4687, URL <https://doi.org/10.1038/nature03081>.
 - ¹³ A. V. Balatsky, Y. N. Joglekar, and P. B. Littlewood, *Phys. Rev. Lett.* **93**, 266801 (2004), URL <https://link.aps.org/doi/10.1103/PhysRevLett.93.266801>.
 - ¹⁴ J.-J. Su and A. H. MacDonald, *Nature Physics* **4**, 799 (2008), ISSN 1745-2481, URL <https://doi.org/10.1038/nphys1055>.
 - ¹⁵ D. K. Efimkin, Y. E. Lozovik, and A. A. Sokolik, *Phys. Rev. B* **86**, 115436 (2012), URL <https://link.aps.org/doi/10.1103/PhysRevB.86.115436>.
 - ¹⁶ C. Zhang and G. Jin, *Applied Physics Letters* **103**, 202111 (2013), <https://doi.org/10.1063/1.4831671>, URL <https://doi.org/10.1063/1.4831671>.
 - ¹⁷ J. I. A. Li, T. Taniguchi, K. Watanabe, J. Hone, and C. R. Dean, *Nature Physics* **13**, 751 (2017), 1608.05846.
 - ¹⁸ Z. Wang, D. A. Rhodes, K. Watanabe, T. Taniguchi, J. C. Hone, J. Shan, and K. F. Mak, *Nature* **574**, 76 (2019), ISSN 1476-4687, URL <https://doi.org/10.1038/s41586-019-1591-7>.
 - ¹⁹ N. Read and D. Green, *Phys. Rev. B* **61**, 10267 (2000), cond-mat/9906453.
 - ²⁰ E. Fradkin, *Field Theories of Condensed Matter Physics*, *Field Theories of Condensed Matter Physics* (Cambridge University Press, 2013), ISBN 9780521764445, URL https://books.google.de/books?id=x7\6MX4ye_wC.
 - ²¹ T. Kato, *Perturbation theory for linear operators; 2nd ed.*, *Grundlehren der mathematischen Wissenschaften A Series of Comprehensive Studies in Mathematics* (Springer, Berlin, 1976), URL <https://cds.cern.ch/record/101545>.
 - ²² G. E. Blonder, M. Tinkham, and T. M. Klapwijk, *Phys. Rev. B* **25**, 4515 (1982), URL <https://link.aps.org/doi/10.1103/PhysRevB.25.4515>.
 - ²³ G. Vignale and A. H. MacDonald, *Phys. Rev. Lett.* **76**, 2786 (1996), cond-mat/9510043.
 - ²⁴ S. Das Sarma, M. Freedman, and C. Nayak, *Phys. Rev. Lett.* **94**, 166802 (2005), URL <https://link.aps.org/doi/10.1103/PhysRevLett.94.166802>.
 - ²⁵ Y. Ji, Y. Chung, D. Sprinzak, M. Heiblum, D. Mahalu, and H. Shtrikman, *Nature* **422**, 415 (2003), ISSN 1476-4687, URL <https://doi.org/10.1038/nature01503>.
 - ²⁶ A. R. Akhmerov, J. Nilsson, and C. W. J. Beenakker, *Phys. Rev. Lett.* **102**, 216404 (2009), URL <https://link.aps.org/doi/10.1103/PhysRevLett.102.216404>.
 - ²⁷ J. A. Sauls, *Philosophical Transactions of the Royal Society of London Series A* **376**, 20180140 (2018), 1805.11069.